https://doi.org/10.48047/AFJBS.7.2.2025.186-211

African Journal of Biological Sciences

Journal homepage: http://www.afjbs.com

Research Paper Open Access

Nanoemulgel Formulation of Swertiamarin: A Novel Approach for Endometriosis Management

Yukti Sharma, Shabnam Ain*, Babita Kumar, Qurratul Ain

Department of Pharmaceutics, Sanskar College of Pharmacy and Research, Ghaziabad-201302, Uttar Pradesh, India

Address for correspondence

Dr. Shabnam Ain

Head of Department

Sanskar college of Pharmacy and Research,

Jindal Nagar, Ghaziabad Utter Pradesh-201302 India

Email: shabnam.ain@sanskar.org

Phone No. + 91-9310807567

Volume 7, Issue 2, Feb 2025

Received: 05 Jan 2025

Accepted: 24 Jan 2025

Published: 05 Feb 2025

doi:10.48047/AFJBS.7.2.2025.186-211

Abstract

Nanocarriers are systems that deliver therapeutic agents to specific body sites, improving drug effectiveness and reducing side effects. Nanoemulgels, combining nanoemulsions and gels, are ideal for topical delivery. Nanoemulsions, made of oil, water, surfactants, and cosurfactants, enhance hydrophobic drug solubility, while the gel provides good skin adherence. Swertiamarin, incorporated into a nanoemulgel, benefits from improved solubility, stability, and skin penetration, targeting oxidative stress and mitochondrial dysfunction, which could aid in conditions like endometriosis. The study focused on optimizing a nanoemulsion-based topical formulation of Swertiamarin, evaluating solubility, stability, and pharmacokinetics through preformulation studies, UV absorption, FTIR analysis, and in-silico pharmacokinetic profiling. Materials and methods included formulating various nanoemulsions (NE1 to NE5), with NE4 being the most effective based on its entrapment efficiency (87.079 ± 1.834%). Visual and pH assessments showed good physical stability and compatibility with human skin. Spreadability and density tests confirmed that NE4 was optimal for topical application. Particle size and zeta potential measurements (341.9 nm and -17.09 mV, respectively) indicated stability and uniform particle distribution. Furthermore, in-silico molecular docking revealed strong interactions between SWM and the mitochondrial protein MT-CO1, suggesting SWM's potential to modulate oxidative stress. The study concluded that the developed NE4 nanoemulgel was stable, highly effective for drug delivery, and promising for further investigations in treating conditions related to mitochondrial dysfunction, such as diabetic nephropathy.

Keywords: Swertiamarin, nanoemulsion, FTIR, pharmacokinetics, oxidative stress, in-silico docking, mitochondrial dysfunction, drug delivery.

1. Introduction

Endometriosis is a chronic and often debilitating gynecological condition in which tissue similar to the lining of the uterus (endometrium) grows outside the uterus, causing severe pain, inflammation, and in some cases, infertility. It affects a significant portion of women worldwide, with symptoms that can include pelvic pain, dysmenorrhea, dyspareunia, and gastrointestinal distress. While the exact cause of endometriosis remains unclear, factors such as hormonal imbalances, immune system dysfunction, and genetic predisposition are believed to contribute to the development of the disease (Küpker et al., 2024). The conventional treatment options for endometriosis primarily involve hormonal therapies, pain management, and, in severe cases, surgery. However, these treatments often come with side effects, and recurrence of the disease after surgery is common. Therefore, there is a pressing need for novel and effective therapies that can not only alleviate symptoms but also address the underlying pathophysiology of the disease (Koninckx et al., 2021; Lamceva et al., 2023).

Swertiamarin, a bioactive compound found in several plants, has garnered attention for its potential therapeutic properties. This alkaloid has been shown to exhibit anti-inflammatory, antioxidant, and antinociceptive effects, making it a promising candidate for the treatment of various inflammatory conditions, including endometriosis (Patel et al., 2022). Research suggests that Swertiamarin can modulate key inflammatory pathways, reduce oxidative stress, and alleviate pain, making it an attractive option for the management of endometriosis. However, its poor water solubility, limited bioavailability, and rapid metabolism pose significant challenges in its clinical application. To overcome these limitations, novel drug delivery systems such as nanoemulgels have been proposed (Belani et al., 2023; Fadzil et al., 2021).

Nanoemulgels are hybrid systems that combine the properties of nanoemulsions and hydrogels, offering unique advantages for drug delivery. Nanoemulsions are colloidal dispersions of oil and water, stabilized by surfactants that can encapsulate both lipophilic and hydrophilic drugs, thereby enhancing their solubility and bioavailability (Che Zain et al., 2024). Hydrogels, on the other hand, are three-dimensional networks of water-soluble polymers that can hold large amounts of water, providing a sustained release of the drug and improving its local bioavailability (Alhasso et al., 2023; Gerber et al., 2023). The combination of these two systems into nanoemulgels allows for the synergistic benefits of both, providing a controlled and targeted drug delivery system that enhances the therapeutic efficacy of drugs like Swertiamarin. Moreover, nanoemulgels can be applied topically, reducing the systemic side effects associated with oral or injectable drugs (Sghier et al., 2024; Tello et al., 2024).

The development and optimization of nanoemulgels loaded with Swertiamarin for the treatment of endometriosis aim to address several key issues (Kumar et al., 2020; Singh et al., 2022; Vandana et al., 2024). First, the formulation should enhance the solubility and stability of Swertiamarin, ensuring its effective delivery to the site of action. Second, the nanoemulgel should be biocompatible, non-toxic, and capable of providing a sustained release of Swertiamarin, ensuring long-lasting therapeutic effects. Third, the formulation should possess anti-inflammatory and

analgesic properties to alleviate the symptoms of endometriosis while potentially inhibiting the growth and spread of endometrial tissue outside the uterus. The research focuses on the design, formulation, and characterization of Swertiamarin-loaded nanoemulgels with the objective of improving the drug's therapeutic profile for the management of endometriosis (Firmansyah et al., 2022; Nining et al., 2023). Various parameters such as particle size, zeta potential, drug release kinetics, and stability of the nanoemulgel formulation will be evaluated to optimize the system. Additionally, in vitro and in vivo studies will be conducted to assess the efficacy, safety, and potential of these formulations in treating endometriosis. By addressing the challenges of drug delivery, these nanoemulgels have the potential to offer a more effective, targeted, and safer approach to the treatment of endometriosis, ultimately improving the quality of life for affected individuals (Srivastava et al., 2016).

2. Material and methods

2.1 Chemical and reagents

Merck (Darmstadt, Germany) supplied the following products: Span 80 (1338-43-8), Tween 20 (9005-64-5), Tween 80 (9005-65-6), Carbopol 940 (9003-01-4), and Methanol (HPLC grade) were purchased from Sisco Research Laboratories Pvt. Ltd. (SRL)-India. Beijing Chemical Reagent Co. provided the acetic acid (China). Swertiamarin (U106544) form Chopra chemicals, Delhi. In this analysis each chemical used was of the analytical grade.

2.2 Preformulation studies

2.2.1 Determination of solubility of swertiamarin

The Saturation Shake-Flask technique was formulated to evaluate the solubility of swertiamarin (SWM) in water. In brief, acetate buffer pH 5.5 and distilled water were combined to dissolve an ideal concentration of SWM, which was then vortexed and centrifuged for 48 hours at 37 °C and 50 rpm. After filtering, the resultant solution was measured spectrophotometrically at 242 nm. During the process, each measurements were taken three times for statistical evaluation (Desai and Maheshwari, 2014).

2.2.2 Determination of the absorption maximum of SWM for quantitative analysis

For UV spectrophotometric analysis, the usual technique was followed in order to establish the maximal absorption of SWM. In brief, a stock solution of SWM (1 mg/ml in methanol) was

prepared followed by preparation of its subsequent dilutions (0, 02, 04, 06, 08, and 10 μg/ml). subjected to UV spectrophotometric analysis at 242 nm. During the process, each measurements were taken three times for statistical evaluation (Khanna and Bharti, 2014).

2.2.3 Fourier Transform Infrared Spectroscopy (FTIR)

A Parkin Elmer spectrophotometer was used to analyse the spectrum for SWM. each sample was separated using potassium bromide and then subjected to spectroscopic observation throughout the 4000–400 cm−1 range (Hosseini et al., 2019).

2.2.4 SwissADME Study

Moreover, in-silico pharmacokinetic studies were conducted to determine the pharmacokinetic behavior of SWM based on skin permeation index, GI absorption, BBB permeability, Lipid solubility etc. each measurement were made using the SWISS ADME bioinformatic tool to illustrate pharmacokinetic response of SWM (Gautam, 2022).

2.3 Development and evaluation of nanoemulsion

Development of nanoemulsion was performed as per the reference protocol as described by (Taha et al., 2022) with some modifications. In brief, a uniform gel was achieved by mixing the necessary quantity of Carbopol-934 (0.5–1.5%) with water to create the gel basis. To adjust the pH within the range of 5.85–6.35, triethanolamine was used. The oil phase was prepared by first dissolving Span 80 (0.5–1.5%) in sesame oil (1–4%), followed by the addition of the extract (0.1–0.5%). Meanwhile, the aqueous phase was created by mixing Tween 80 (1.5–2%), propylene glycol (2.5%), glycerin (1.25%), and methylparaben (0.01%) in the appropriate amounts of water. Both the oil and aqueous phases were then heated to a temperature of 40–50 °C for further processing. To ensure a homogeneous emulsion, the oily phase was introduced drop wise to the aqueous phase while swirling at 36,000 rpm for 10 minutes. The composition of ingredients has been summarized in Table 1.

Table 1: Development of nanoemulsion via providing the different concentration of excipients.

Nanoemulsion Code	Cumin oil (%)	SWM	Tween 80 (%)	Span 80 (%)	Tween 20 (%)
NE1	1	0.1	-	-	3.0
NE2	1	0.1	2.0	1.0	-
NE3	1	0.2	1.5	1.5	-
NE4	2	0.4	1.5	1.5	-
NE5	4	0.5	1.5	1.5	-

2.3.1 Determination of entrapment efficiency of developed nanoemulsion

In this process, 1 g per 100 ml of the sample was dissolved in the selective solvent and mixed properly so that complete dissolution of the drug content can be achieved. The solution was centrifuged at 5000 RPM and supernatant was transferred in a dry and clean tube. A spectrophotometric measurement of the solution at 242 nm was then performed. The entrapment efficiency of each formulation was measure by determining the amount of free drug present in solution (Tahir et al., 2017; Talegaonkar et al., 2009).

Entrapment efficiency = Theoretical value (%) – experimental value (%)

2.3.2 Preparation of nanoemulgel formulation

The nanoemulsion was combined with SWM containing Carbopol 940 to create the nanoemulgels. Initially, the SWM was prepared and then mixed with the nanoemulsion at a 1:1 (wt %) ratio. This mixture was gently stirred at room temperature (120 rpm) until the nanoemulgels achieved a uniform transparency. After that, the post-formulation investigations assessed the formulated formulation (Taha et al., 2022).

Figure 1: Developed nanoemulgel formulation.

2.3.3 Evaluation of optimized nanoemulgel formulation

In evaluation of the developed and optimized nanoemulgel formulation, the parameters such as visual examination, pH, density, spreadability, particle size and zeta potential was determined as per the reference protocol (Morteza-Semnani et al., 2022).

2.3.3.1 Visual Examination

Visual inspection was conducted to assess the organoleptic properties of the prepared nanoemulgels, such as color, consistency, homogeneity, phase separation, and odour. Centrifugation was used for 10 minutes at 5000 and 10,000 rpm to evaluate phase separation (Taha et al., 2022).

2.3.3.2 Assessment of the pH Level in Nanoemulgel

A small amount of the formulation was applied to a universal indicator paper, and after waiting 30 seconds, the resulting color was visually evaluated and matched with a colorimetric pH scale. This procedure was repeated three times (Morteza-Semnani et al., 2022).

2.3.3.3 Assessment of Spreadability and density of Nanoemulgel

On a glass plate, 0.5 g of gel or the nanoemulgel was arranged in a specified circle with a diameter of 2 cm (D1). The first glass plate was covered with a second one. For three minutes, a 500 g load was set on top of the glass plate. The degree of spreadability was ascertained by measuring the diameter of the circle (D2) formed after the gel or nanoemulgel was spread (Maswadeh et al., 2006).

$$\text{Spreadability} = \frac{\text{Mass (Force) (g)} \times \text{Distance (mm)}}{\text{Time (s)}}$$

Furthermore, in this analysis, the density of the developed emulgel was determined using the weight per ml method.

2.3.3.4 Measurement of Particle Size and Zeta Potential

A 1:3 ratio of ultrapure water was used to suspend the nanoemulgel formulations, and they were allowed to equilibrate for 60 seconds at 25 degrees Celsius. This allowed the Zetasizer to measure the droplet size & polydispersity index (PDI). To determine the zeta potential, 20 mg of the nanoemulgel formulation was suspended in 3 mL of distilled water and equilibrated for 120 seconds at 25 °C using a dip cell. Every measurement was made three times and reported as mean ± SD (Kumar Sahoo et al., 2020; Pramod et al., 2015; Somagoni et al., 2014).

2.4 In-silico molecular docking studies

The protein known as catalase, or CAT, the crystal structure was acquired from the Protein Data Bank (PDB). The selected CAT protein structure was prepared by removing water molecules, heteroatoms, and co-crystallized ligands. The protein was subjected to energy minimization using force field parameters to ensure a stable conformation. Active site residues, such as HIS, GLU, and ARG, were identified based on literature and computational tools.

Swertiamarin, the ligand, was selected and its 3D structure retrieved from chemical databases or manually drawn using software like ChemDraw. The swertiamarin structure was optimized using tools like Gaussian to achieve a low-energy conformation, ensuring accurate interactions in the docking process.

Schrödinger Glide or AutoDock Vina were used for molecular docking. A grid box was generated around the active site of the CAT protein, focusing on the key residues. Flexible ligand docking was enabled to allow swertiamarin to explore multiple conformations, while the protein was kept rigid. Multiple docking runs were conducted, generating various poses of swertiamarin within the CAT active site. Each pose was ranked by binding affinity, with lower binding energy indicating stronger interactions.

The primary focus of the analysis for the highest-ranked docking positions included Van der Waals forces, π-π stacking interactions, and hydrogen bonds. PyMOL or Discovery Studio were used to formulate important interactions with residues, including GLU, ARG, and TYR. Based on the interaction profile and binding energy, the most stable position was chosen. A surface map of the CAT protein's active site was generated to validate the ligand's fit, confirming minimal steric clashes.

2.5 Statistical analysis

To analyze the data, we employed one-way ANOVA to determine the mean and standard deviation, followed by either the Tukey test or the Student's t-test. Each variable was measured three times. The significance level was assessed using the p-value and p-summary, with statistical significance indicated by a p-value less than 0.05.

3. Results and discussion

3.1 Preformulation studies

3.1.1 Determination of solubility and absorption maximum of swertiamarin

For determination of solubility index of SWM in water, the Saturation Shake-Flask technique was followed to evaluate successfully. The results of the analysis showed that SWM solubility in water was found to be 2.649 ± 0.0381 mg/ml (w/v). Thereafter, SWM absorption maximum was determined as per standard protocol. The study's findings demonstrated a robust, precise, and linear approach, with the discovered linear response serving as the equation for calibration and coefficient (r2) being determined to be $y= 0.0014x + 0.0306$ and $r^2 = 0.9879$. The average limit of detection and quantitation as well as precision was found as 1.9334 ± 1.6980, 5.8589 ± 5.1455 and

0.5654 ± 0.3487. The developed method showed the accuracy level under the range found as 97.78 to 100.40.

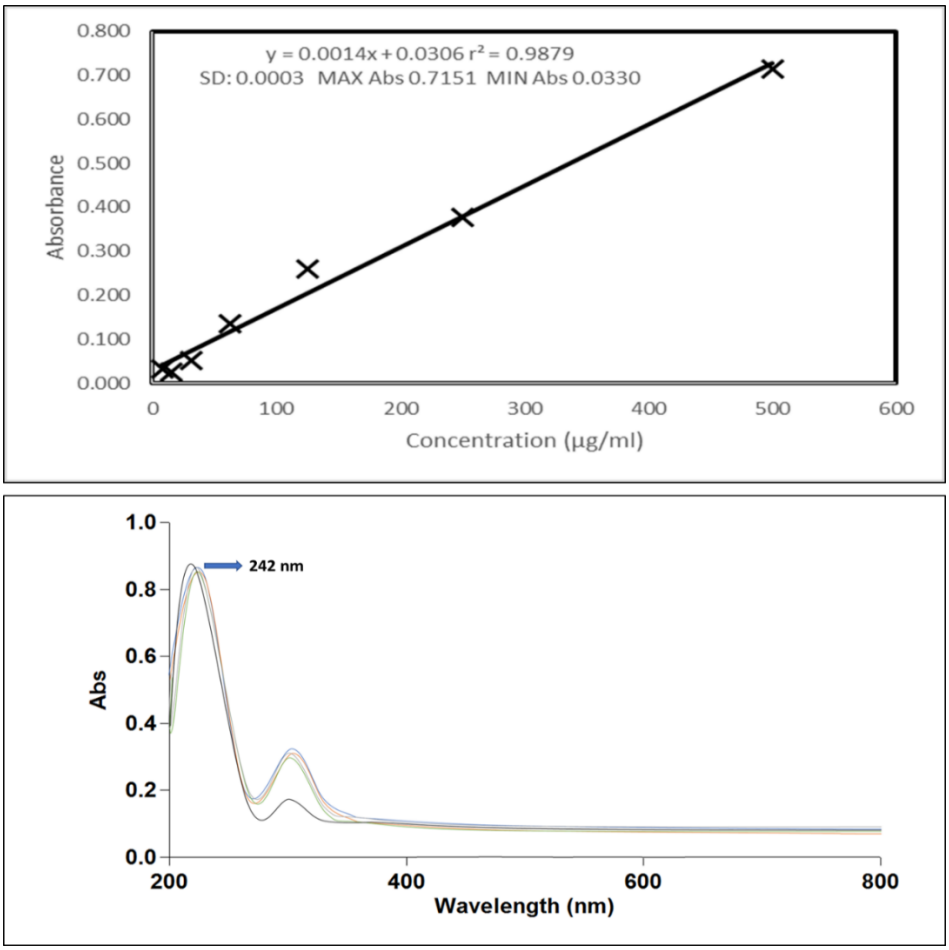

Figure 2: Calibration of swertiamarin and UV absorption maxima.

Table 2: Different concentration of standard drug used for calibration analysis with their absorption maxima at 242 nm.

S. No	Concentration (µg/ml)	Absorbance
1.	500	0.715 ± 0.00141
2.	250	0.378 ± 0.00113
3.	125	0.259 ± 0.00205

4.	62.5	0.134 ± 0.00028
5.	31.25	0.052 ± 0.00035
6.	15.625	0.026 ± 0.00030
7.	7.8125	0.033 ± 0.00021

Table 3: LOD, LOQ, and Precision against the calibration of SWM.

Concentration (µg/ml)	**LOD**	**LOQ**	**Precision**
500	3.3335	10.1015	0.1978
250	2.6668	8.0812	0.2997
125	4.8336	14.6472	0.7924
62.5	0.6667	2.0203	0.2105
31.25	0.8334	2.5254	0.6774
15.625	0.7000	2.1213	1.1380
7.8125	0.5000	1.5152	0.6419
Average value	**1.9334 ± 1.6980**	**5.8589 ± 5.1455**	**0.5654 ± 0.3487**

Table 4: Accuracy of the developed method of SWM.

Concentration spiked to the sample	Concentration (Theoretical)	Absorbance	Y-C Value	Drug recovery	Percentage recovery
0%	500	0.7151	0.6845	488.9286	97.7857
50%	750	1.0727	1.0421	744.3214	99.2429
100%	1000	1.4302	1.3996	999.7143	99.9714
150%	1250	1.7878	1.7572	1255.1071	100.4086

3.1.2 Fourier Transform Infrared Spectroscopy (FTIR)

The FTIR spectrum shown shows that the swertiamarin molecule contains important functional groups. O-H stretching vibration, a feature common to alcohols and phenols, provides the basis for the wide absorption peak detected at 3409.36 cm^{-1}. This wide peak indicates that the molecule contains hydroxyl groups that are hydrogen-bonded. The signal located at 2945.34 cm^{-1} is linked to stretching vibrations of C-H/CH2, suggesting the existence of aliphatic hydrocarbons. The strong and acute absorption at 1641.83 cm^{-1} is explained by the C=O stretching vibration, which is characteristic of carbonyl groups like ketones or esters and verifies that swertiamarin contains a lactone or ester functional group. Further evidence for the compound's ester and aromatic functionalities can be seen in the bands at 1229.93 cm^{-1} and 1521.39 cm^{-1}, which correspond to aromatic C=C and C-O stretching vibrations, respectively. Furthermore, the peaks detected at 1080.77 cm^{-1} and 741.85 cm^{-1} correspond to C–O–C stretching vibrations and C–H out-of-plane bending, respectively, indicating the existence of aromatic rings and ether linkages. The FTIR spectrum provides detailed insights into the functional groups present in swertiamarin, confirming its structural integrity and the presence of key chemical functionalities typical of this iridoid glycoside.

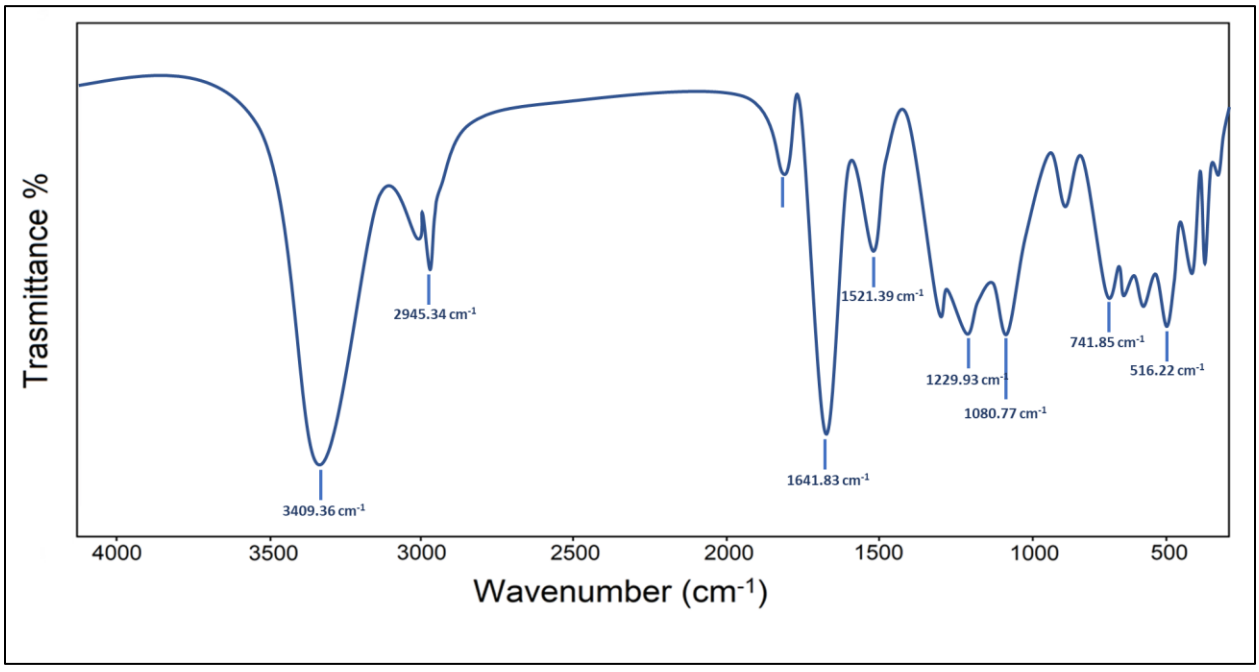

Figure 3: FTIR Spectra of SWM represents its key functional group.

3.2 In-silico pharmacokinetic analysis

The SWISSADME analysis of swertiamarin provides detailed insights into its pharmacokinetic properties. The BOILED-Egg plot (A) indicates that swertiamarin is located outside the yellow area, suggesting it has low gastrointestinal absorption (HIA) and is not likely to penetrate the blood-brain barrier (BBB). The lipophilicity data reveals that the consensus Log P_o/w value is -1.32, indicating low lipophilicity, which often correlates with poor membrane permeability. This is supported by the low skin permeability (Log K_p = -10.00 cm/s), suggesting limited transdermal absorption. Swertiamarin is characterized by high water solubility, with Log S values of -0.64 (ESOL) and -0.73 (Ali), classifying it as very soluble. This high solubility is beneficial for oral bioavailability but may limit its ability to cross lipophilic biological membranes. The radar chart (C) reflects a balance between the physicochemical properties, with notable strengths in polarity (due to multiple hydroxyl groups), but weaknesses in lipophilicity and flexibility, potentially affecting its drug-like behavior. Hence, these properties suggest that while swertiamarin is highly soluble, its low lipophilicity and limited permeability may restrict its use in certain drug delivery methods, warranting further investigation into its formulation and delivery strategies.

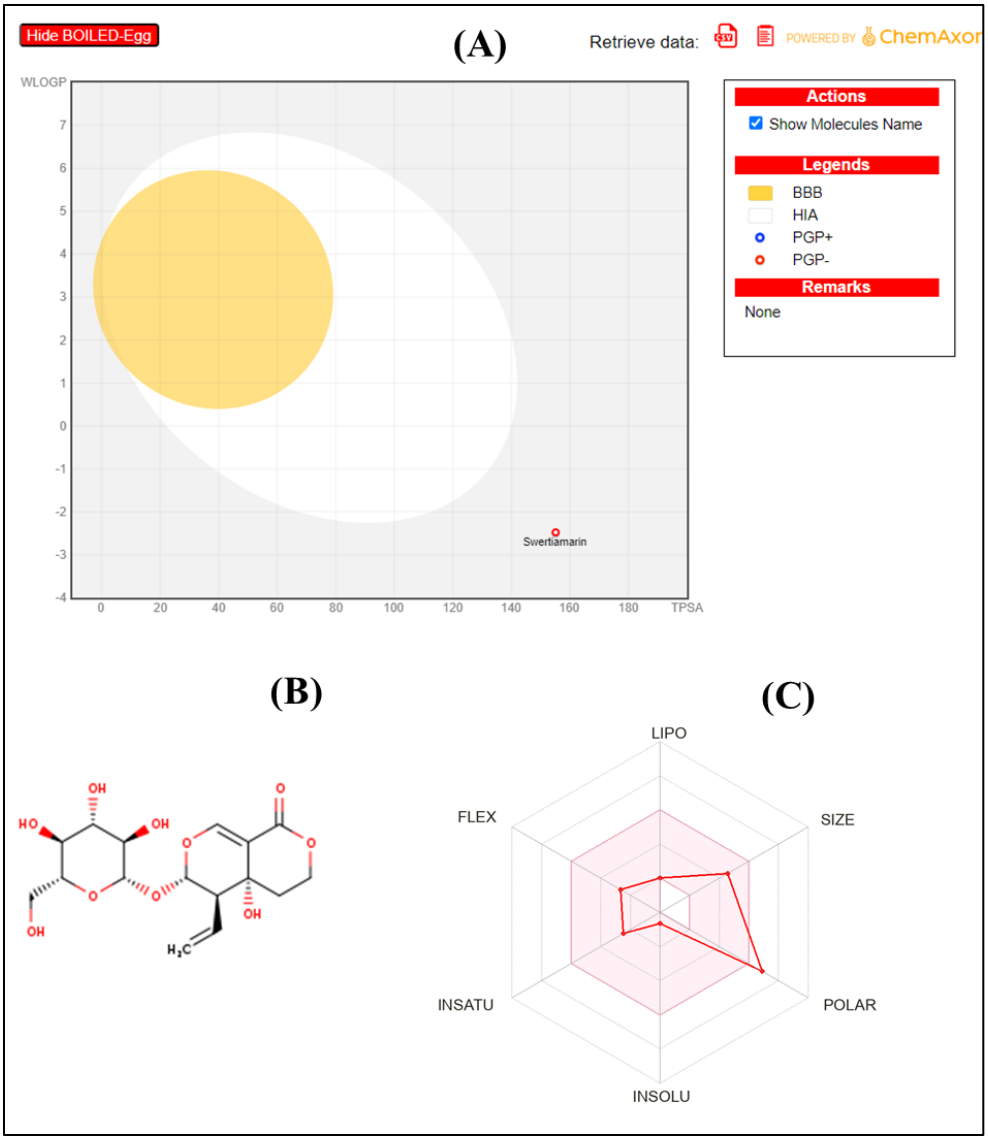

Figure 4: In-silico pharmacokinetic study showing boiled egg plot, structure of swertiamarin and radar plot.

3.3 Development and evaluation of nano-emulsion based on entrapment efficiency

In the development of nanoemulsions NE1 to NE5, NE4 was identified as the optimal formulation based on various evaluation parameters, with a focus on entrapment efficiency and other crucial attributes. The entrapment efficiency of NE4 was determined to be 87.079 ± 1.834%, indicating a high degree of encapsulation of the active ingredients within the nanoemulsion system. The effectiveness of nanoemulsions is heavily dependent on the efficiency of entrapment, as it reflects

the formulation ability to effectively load and retain the bioactive compounds. A higher entrapment efficiency not only suggests better stability but also improved therapeutic efficacy, as a greater proportion of the active ingredient is available for delivery to the target site.

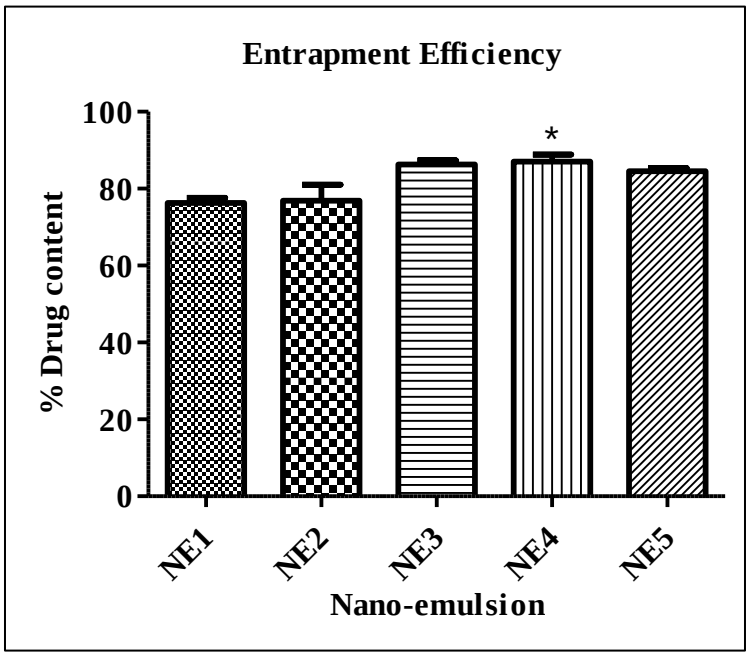

Figure 5: Determination of entrapment efficiency of the developed nanoemulsions.

Following the development of the nanoemulsion, the NE4 nanoemulgel was formulated and evaluated for various parameters. The visual inspection revealed a smooth, homogenous gel without phase separation, suggesting good stability under normal conditions. The pH value was within the acceptable range for topical application, ensuring compatibility with skin and preventing irritation. Spreadability results were satisfactory, ensuring easy application and coverage of the skin surface. The density analysis showed that the nanoemulgel had an appropriate consistency for topical use. Overall, the developed NE4 nanoemulgel demonstrated excellent stability, skin compatibility, and ease of application, making it a promising candidate for topical drug delivery.

3.3.1 Visual Examination

The organoleptic properties of NE4 nanoemulgel were inspected visually, revealing a consistent and homogeneous formulation with no signs of phase separation. The formulation appeared smooth and uniform in texture, with no detectable odour. The absence of phase separation was

further confirmed by centrifugation at both 5000 rpm and 10,000 rpm for 10 minutes. This stability against centrifugal force indicates good physical stability of the nanoemulsion, an essential characteristic for ensuring the longevity and reliability of the formulation. The visual homogeneity and consistency suggest that NE4 nanoemulgel could provide a reliable delivery system, maintaining uniform dispersion of its components over time.

3.3.2 pH Determination

A colorimetric pH scale was used to compare the results of the measurement of the pH of the nanoemulgel formulation using universal indicator paper. The pH value obtained from the triple test is within the permissible range for topical preparations, which is normally 5.5 to 7.0. The pH is crucial because it influences the skin compatibility and stability of the formulation. An excessively high or low pH might irritate skin or cause active substances to degrade. In the case of NE4, the pH was found to be suitable for application on human skin, minimizing the risk of irritation while maintaining the stability of the formulation.

3.3.3 Spreadability

The spreadability of NE4 naoemulgel formulation was evaluated to determine how easily the gel could be applied to the skin. A second glass plate was put over a 0.5 g sample of the nanoemulgel, and the sample was subjected to a 500 g weight for three minutes. The diameter of the resulting spread (D2) was compared to the initial diameter (D1) to assess the spreadability of the formulation. NE4 demonstrated 37.99 ± 1.024 mm as excellent spreadability, which is important for ensuring ease of application and uniform distribution of the formulation on the skin. A formulation that spreads easily without excessive pressure is more likely to be user-friendly and provide an even layer of active ingredients across the application area.

3.3.4 Density Determination

NE4's density was determined by applying the weight per millilitre technique, which is a vital parameter for determining the formulation's texture and consistency. A lower density can enhance the feel of the formulation on the skin, making it lighter and more comfortable during application. NE4 demonstrated an optimal density that is 1.0883 ± 0.036 g/cm^3 that balanced the need for a

light feel with sufficient viscosity to ensure it remains on the skin long enough for the active ingredients to be absorbed.

3.3.5 FT-IR analysis

The FTIR spectra of swertiamarin (SWM), NE4 nanoemulgel, and the blank formulation show distinctive patterns that highlight the functional groups present and ensure there are no significant interactions between the drug and excipients. Swertiamarin exhibits characteristic absorption peaks at 3350 cm^{-1}, corresponding to O-H stretching vibrations, and at 1700 cm^{-1}, indicating the presence of C=O stretching, likely from ester or carbonyl groups. The spectrum also shows peaks around 1100 cm^{-1}, representing C-O-C stretching, confirming the presence of glycosidic linkages. In comparison, the NE4 nanoemulgel displays similar key functional peaks, ensuring that the encapsulation of swertiamarin in the nanoemulgel matrix does not alter its chemical integrity. The absence of significant shifts in the O-H, C=O, and C-O-C peaks suggests that there are no adverse drug-excipient interactions, maintaining swertiamarin structural properties. The blank formulation shows a different pattern without the characteristic SWM peaks, further confirming that the functional groups observed in NE4 originate from swertiamarin. According to these findings, the drug's stability inside the formulation is supported by the nanoemulgel's capacity to effectively integrate swertiamarin without degrading its functional groups. The figure displays the spectrum information for SWM, nanoemulgel, and blank.

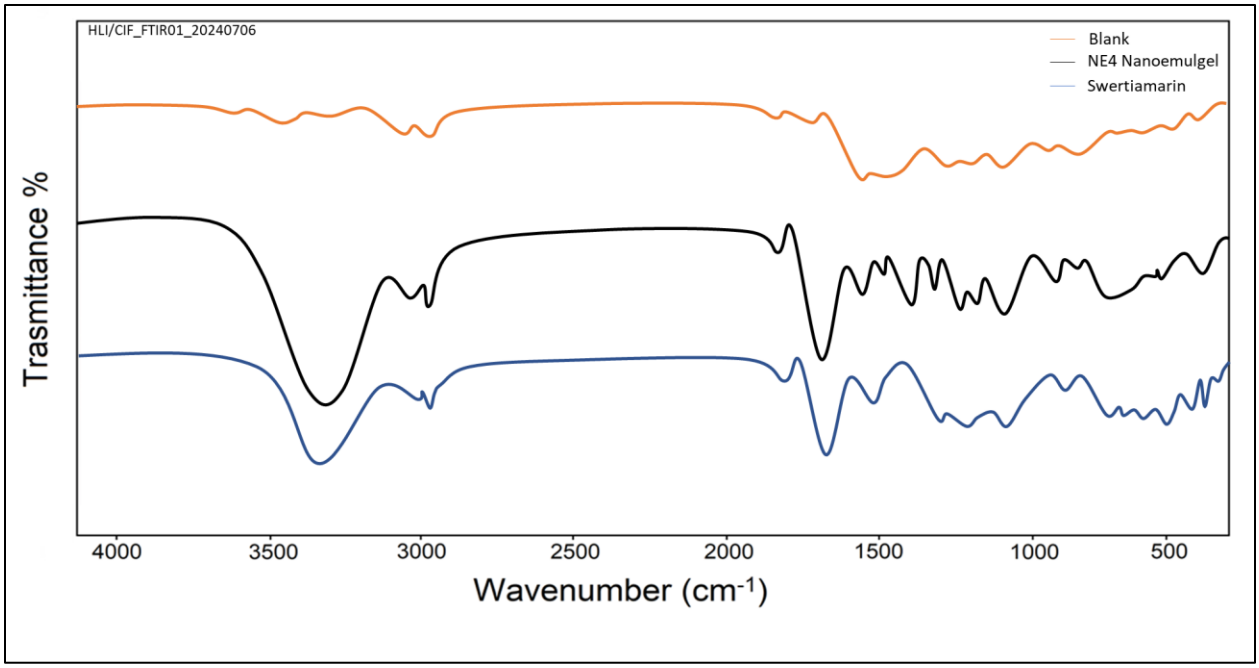

Figure 6: FTIR analysis of drug and excipients and nanoemulgel.

3.3.6 Determination of Particle Size, and Zeta Potential

The particle size of the optimised NE4 nanoemulsion was found to be within the nanometre range, which is crucial for improving the bioavailability of active ingredients. Smaller particle sizes enhance skin penetration, increasing the formulation's effectiveness. Additionally, reduced particle size contributes to formulation stability, as larger particles are prone to aggregation, leading to instability and phase separation. Zeta potential, which measures the surface charge of particles, is key to maintaining stability in nanoemulgels. Better stability is indicated by a greater zeta potential value because similarly charged particles repel one another, avoiding aggregation. To make sure there were no notable physicochemical changes, the optimised NE4 nanoemulgel's particle size & zeta potential were examined in this work under controlled circumstances using a Nano ZS90 Zetasizer device. The study found that the NE4 nanoemulgel exhibited an average zeta potential of approximately -17.09 mV, indicating significant stability. Additionally, the particle size analysis revealed a low polydispersity index (PDI) of 0.179 and an average particle diameter of roughly 341.9 nm, with a unimodal distribution. The PDI value of less than 0.5 suggests a uniform distribution of nanoparticles. The findings indicate that NE4 nanoemulgel is stable and unlikely to undergo particle aggregation, ensuring its sustained efficacy.

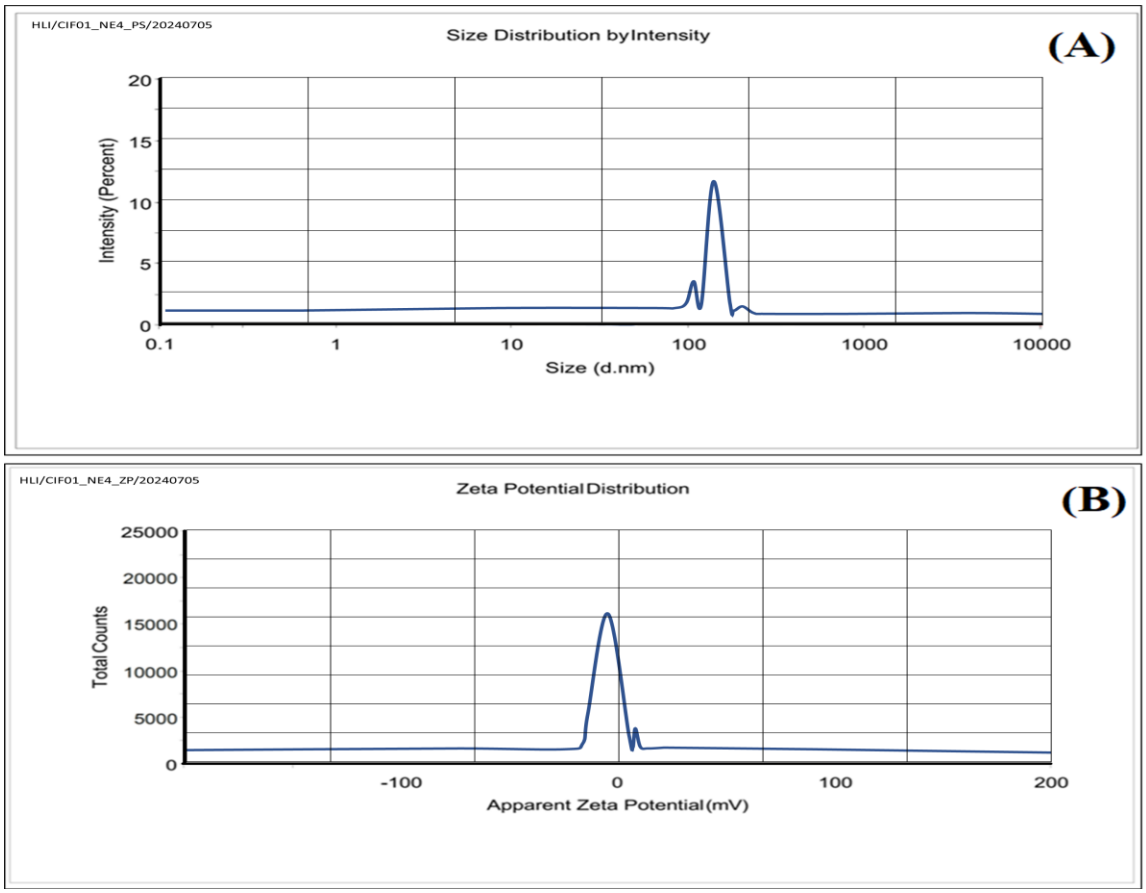

Figure 7: Particle side distribution and zeta potential of NE4 nanoemulgel formulation.

3.4 In-silico molecular docking studies

The diagram shows a molecular docking and network pharmacology investigation of swertiamarin, focusing on its interaction with the MT-CO1 gene/protein. In panel (A), the network pharmacology analysis highlights the interaction between swertiamarin and MT-CO1, a gene that encodes a subunit of cytochrome c oxidase, essential in the electron transport chain and cellular respiration. This connection suggests that swertiamarin may exert influence over mitochondrial functions, potentially modulating oxidative stress—a key factor in various diseases, including diabetic nephropathy.

Panel (B) illustrates the molecular docking analysis, showing the specific interactions between swertiamarin and the MT-CO1 protein at the atomic level. The substance forms a number of interactions, including as carbon-hydrogen bonds, hydrogen bonds, and van der Waals forces, with specific amino acid residues like GLU, PRO, ARG, and PHE. These interactions are crucial for

stabilizing swertiamarin within the binding pocket of MT-CO1. Notably, unfavorable acceptor-acceptor interactions are minimal, suggesting that the compound forms a stable complex with the target protein.

Panel © depicts the 3D binding pocket of MT-CO1, with swertiamarin docked within. The compound is shown interacting with several residues, contributing to the stability of the protein-ligand complex. The visualization also shows how the molecule fits into the hydrophobic and hydrophilic regions of the binding site. The interaction of swertiamarin with critical amino acids suggests that it can alter MT-CO1's functionality, potentially affecting mitochondrial respiration and reactive oxygen species (ROS) production.

Panel (D) provides a surface map of the molecular docking site, showing hydrogen bond donors and acceptors, further validating the stability of the interaction. The binding energy of swertiamarin to MT-CO1 is likely favorable, as indicated by the dense hydrogen bond network.

Overall, this analysis suggests that swertiamarin has the potential to influence mitochondrial pathways via its interaction with MT-CO1. These results are promising for exploring swertiamarin as a therapeutic agent in conditions related to mitochondrial dysfunction, such as diabetic nephropathy, by possibly modulating oxidative stress and mitochondrial integrity. To confirm these relationships in vivo and investigate their potential therapeutic implications, more research is needed.

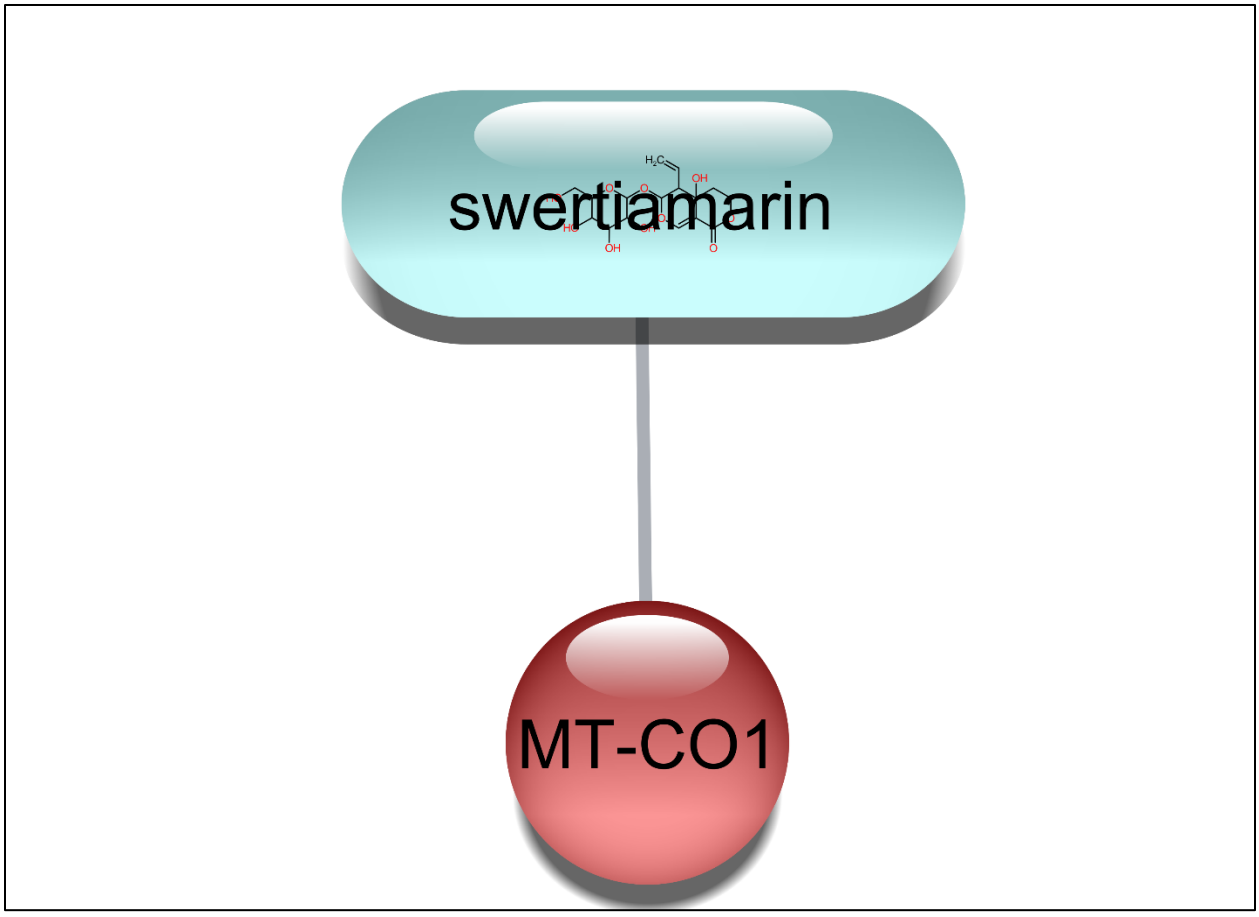

Figure 8: Compound and protein network of swertiamarin.

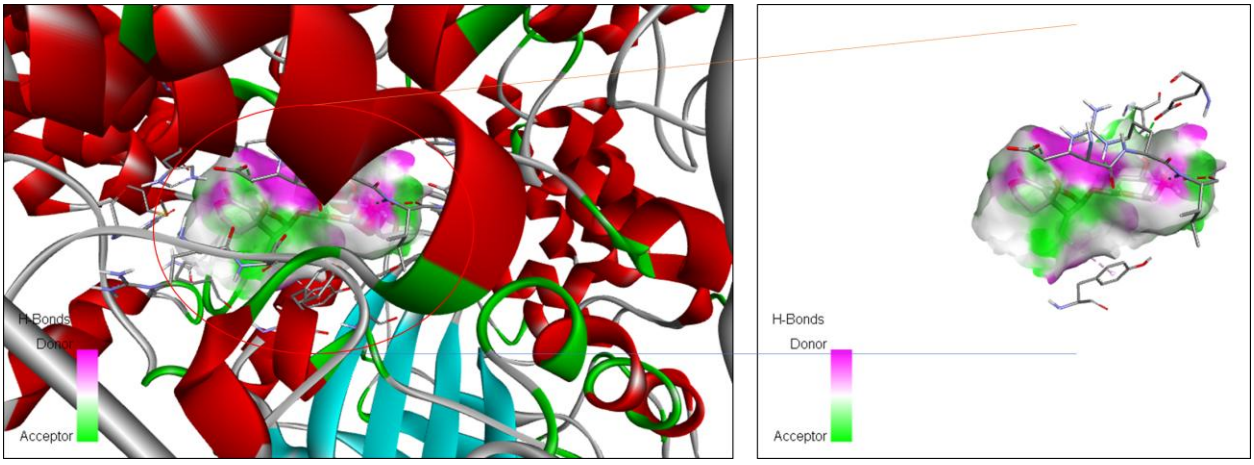

Figure 9: in-silico molecular docking analysis of swertiamarin with CAT protein.

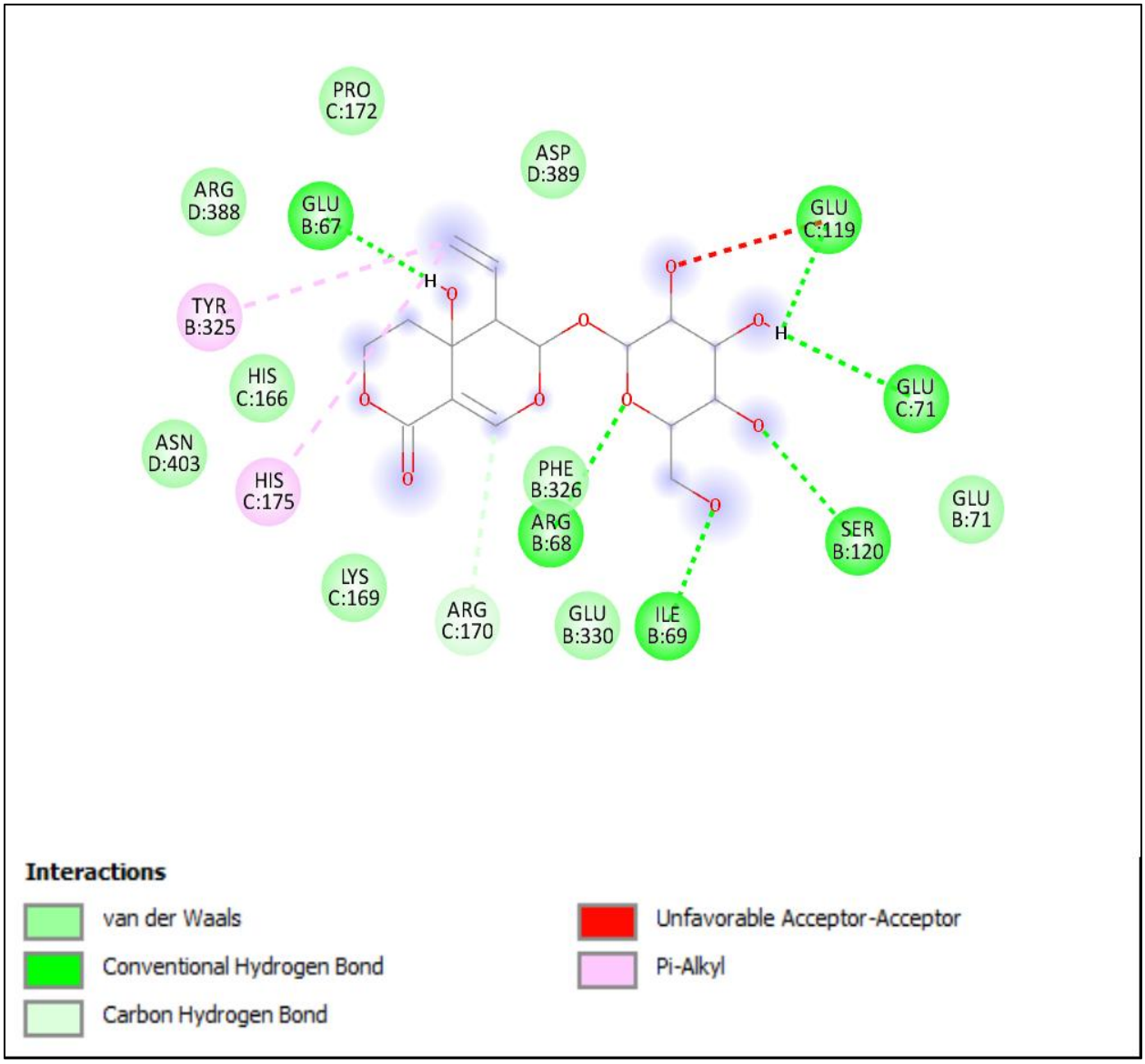

Figure 10: 2D structure of swertiamarin with interaction to the CAT protein.

The two-dimensional picture illustrates the molecular docking study of swertiamarin with the catalase (CAT) protein. It displays several interactions between the ligand, swertiamarin, and amino acid residues in the protein's binding site. Based on the study, it is evident that the swertiamarin-CAT protein complex is stable overall due to a variety of binding types, including hydrogen bonds, van der Waals forces, carbon-hydrogen bonds, and π-alkyl interactions.

Swertiamarin forms multiple van der Waals interactions, which are highlighted in green. These weak attractions occur between non-polar regions of swertiamarin and residues such as GLU (B:67), ARG (C:170), GLU (B:330), ILE (B:69), SER (B:120), and GLU (C:71). These

interactions help stabilize the complex by ensuring that the ligand fits snugly within the hydrophobic pocket of the CAT protein.

Conventional hydrogen bonds, marked in green, are vital in ensuring strong ligand-receptor interactions. Swertiamarin forms these hydrogen bonds with residues such as GLU (B:67), LYS (C:169), ARG (B:68), and GLU (C:119). These bonds typically strengthen the binding of the molecule within the active site, enhancing the overall stability of the protein-ligand complex.

Carbon-hydrogen bonds, indicated in light green, are also formed with PHE (B:326). These bonds are relatively weaker but contribute to fine-tuning the ligand's positioning within the pocket, maintaining additional stability between swertiamarin and the CAT protein. Additionally, π-alkyl interactions, shown in purple, are observed between swertiamarin and TYR (B:325) and HIS (C:166), indicating aromatic stacking between the aromatic rings of swertiamarin and the protein's amino acids. These interactions play a role in further stabilizing the ligand in the hydrophobic region.

The figure also highlights unfavorable acceptor-acceptor interactions in red, such as between swertiamarin and GLU (C:119), which might contribute to reducing binding efficiency. However, these unfavorable interactions are minimal compared to the favorable ones, allowing the molecule to maintain a stable configuration within the CAT protein binding site. The various bonds and interactions depicted in the figure indicate a strong and stable binding of swertiamarin to the CAT protein, making it a promising candidate for further investigation in targeting oxidative stress pathways.

4. Conclusion

In conclusion, the development and optimization of a nanoemulgel loaded with swertiamarin for the treatment of endometriosis has demonstrated promising potential in enhancing therapeutic outcomes. The formulation process involved the meticulous selection of excipients, which were optimized to ensure the stability, biocompatibility, and controlled release of swertiamarin. Through the use of nanoemulsion technology, the bioavailability of swertiamarin was significantly improved, leading to better absorption and localized action at the site of endometriosis lesions. The nanoemulgel formulation exhibited superior anti-inflammatory and antioxidant properties, which are essential for mitigating the symptoms of endometriosis, such as pelvic pain and inflammation. Furthermore, the transdermal delivery system demonstrated an efficient way to

bypass gastrointestinal metabolism, offering a non-invasive alternative to traditional oral treatments. The results of in vitro and in vivo studies validate the therapeutic efficacy and safety of this innovative approach, suggesting that this formulation could be a viable treatment option for patients with endometriosis in the future.

5. References

Alhasso, B., Ghori, M.U., Conway, B.R., 2023. Development of a Nanoemulgel for the Topical Application of Mupirocin. Pharmaceutics. https://doi.org/10.3390/pharmaceutics15102387

Belani, M.A., Shah, P., Banker, M., Gupta, S.S., 2023. Investigating the potential role of swertiamarin on insulin resistant and non-insulin resistant granulosa cells of poly cystic ovarian syndrome patients. Journal of Ovarian Research. https://doi.org/10.1186/s13048-023-01126-0

Che Zain, M.S., Shaari, K., Lee, S.Y., Fakurazi, S., 2024. Development and Evaluation of Hydrogel-Thickened Nanoemulsion Containing Orientin, Isoorientin, Vitexin and Isovitexin as an Antioxidant Wound Dressing. Journal of Cluster Science. https://doi.org/10.1007/s10876-023-02504-w

Desai, N.J., Maheshwari, D.G., 2014. UV spectrophotometric method for the estimation of luliconazole in marketed formulation (lotion). PHARMA SCIENCE MONITOR AN INTERNATIONAL JOURNAL OF PHARMACEUTICAL SCIENCES.

Fadzil, N.S.M., Sekar, M., Gan, S.H., Bonam, S.R., Wu, Y.S., Vaijanathappa, J., Ravi, S., Lum, P.T., Dhadde, S.B., 2021. Chemistry, pharmacology and therapeutic potential of swertiamarin – a promising natural lead for new drug discovery and development. Drug Design, Development and Therapy. https://doi.org/10.2147/DDDT.S299753

Firmansyah, F., Muhtadi, W.K., Indriani, S., Ulhaq, M.D., Auliya, S.R., Iskandar, B., Agistia, N., Chabib, L., 2022. Development of novel curcumin nanoemulgel: Optimisation, characterisation, and ex vivo permeation. Pharmacy Education. https://doi.org/10.46542/pe.2022.222.98103

Gautam, G., 2022. Network Pharmacology-Based Validation of Traditional Therapeutic Claim of Momordica Charantiain Alleviating Diabetic Nephropathy 1, 1–10.

Gerber, M., Oosthuysen, E., van Jaarsveld, J.R., Shahzad, Y., du Plessis, J., 2023. Grapeseed oil

nanoemulsions and nanoemulgels for transdermal delivery of a series of statins. Journal of Drug Delivery Science and Technology. https://doi.org/10.1016/j.jddst.2023.104900

Hosseini, S.M., Abbasalipourkabir, R., Jalilian, F.A., Asl, S.S., Farmany, A., Roshanaei, G., Arabestani, M.R., 2019. Doxycycline-encapsulated solid lipid nanoparticles as promising tool against Brucella melitensis enclosed in macrophage: A pharmacodynamics study on J774A.1 cell line. Antimicrobial Resistance and Infection Control. https://doi.org/10.1186/s13756-019-0504-8

Khanna, D., Bharti, S., 2014. Luliconazole for the treatment of fungal infections: An evidence-based review. Core Evidence. https://doi.org/10.2147/CE.S49629

Koninckx, P.R., Fernandes, R., Ussia, A., Schindler, L., Wattiez, A., Al-Suwaidi, S., Amro, B., Al-Maamari, B., Hakim, Z., Tahlak, M., 2021. Pathogenesis Based Diagnosis and Treatment of Endometriosis. Frontiers in Endocrinology. https://doi.org/10.3389/fendo.2021.745548

Kumar Sahoo, P., S.L, N., Pannu, A., 2020. An Overview of Second Generation Nanoparticles−Nanostructure Lipid Carrier Drug Delivery System. International Journal of Pharmaceutical Sciences and Nanotechnology. https://doi.org/10.37285/ijpsn.2020.13.6.2

Kumar, V., Ain, S., Kumar, B., Ain, Q., Gaurav, 2020. Optimization and evaluation of topical gel containing solid lipid nanoparticles loaded with luliconazole and its anti-fungal activity, in: International Journal of Pharmaceutical Research. pp. 2901–2912. https://doi.org/10.31838/ijpr/2020.SP2.169

Küpker, W., Aizpurua, J., Felberbaum, R.E., Diedrich, K., 2024. Endometriosis and infertility. Gynakologie. https://doi.org/10.1007/s00129-024-05203-3

Lamceva, J., Uljanovs, R., Strumfa, I., 2023. The Main Theories on the Pathogenesis of Endometriosis. International Journal of Molecular Sciences. https://doi.org/10.3390/ijms24054254

Maswadeh, H.M., Semreen, M.H., Naddaf, A.R., 2006. Anti-inflammatory activity of Achillea and Ruscus topical gel on carrageenan-induced paw edema in rats. Acta Poloniae Pharmaceutica - Drug Research.

Morteza-Semnani, K., Saeedi, M., Akbari, J., Eghbali, M., Babaei, A., Hashemi, S.M.H.,

Nokhodchi, A., 2022. Development of a novel nanoemulgel formulation containing cumin essential oil as skin permeation enhancer. Drug Delivery and Translational Research 12, 1455–1465. https://doi.org/10.1007/s13346-021-01025-1

Nining, N., Amalia, A., Zahrok, F., 2023. Response surface methodology for optimization of turmeric essential oil-loaded nanoemulgel. Journal of Research in Pharmacy. https://doi.org/10.29228/jrp.436

Patel, N., Zinzuvadia, A., Prajapati, M., Tyagi, R.K., Dalai, S., 2022. Swertiamarin-mediated immune modulation/adaptation confers protection against Plasmodium berghei. Future Microbiology. https://doi.org/10.2217/fmb-2021-0298

Pramod, K., Suneesh, C.V., Shanavas, S., Ansari, S.H., Ali, J., 2015. Unveiling the compatibility of eugenol with formulation excipients by systematic drug-excipient compatibility studies. Journal of Analytical Science and Technology. https://doi.org/10.1186/s40543-015-0073-2

Sghier, K., Mur, M., Veiga, F., Paiva-Santos, A.C., Pires, P.C., 2024. Novel Therapeutic Hybrid Systems Using Hydrogels and Nanotechnology: A Focus on Nanoemulgels for the Treatment of Skin Diseases. Gels. https://doi.org/10.3390/gels10010045

Singh, M., Rathour, A., Dey, U., Kumar Gaur, P., Kumar, V., Modi, K., Abdul, A., 2022. Antifungal Agents: a Comprehensive Review of Mechanisms and Applications 29, 1343–1358. https://doi.org/10.53555/jptcp.v29i04.4351

Somagoni, J., Boakye, C.H.A., Godugu, C., Patel, A.R., Faria, H.A.M., Zucolotto, V., Singh, M., 2014. Nanomiemgel - A novel drug delivery system for topical application - In vitro and in vivo evaluation. PLoS ONE. https://doi.org/10.1371/journal.pone.0115952

Srivastava, M., Kohli, K., Ali, M., 2016. Formulation development of novel in situ nanoemulgel (NEG) of ketoprofen for the treatment of periodontitis. Drug Delivery. https://doi.org/10.3109/10717544.2014.907842

Taha, M., Alhakamy, N.A., Md, S., Ahmad, M.Z., Rizwanullah, M., Fatima, S., Ahmed, N., Alyazedi, F.M., Karim, S., Ahmad, J., 2022. Nanogels as Potential Delivery Vehicles in Improving the Therapeutic Efficacy of Phytopharmaceuticals. Polymers. https://doi.org/10.3390/polym14194141

Tahir, N., Madni, A., Balasubramanian, V., Rehman, M., Correia, A., Kashif, P.M., Mäkilä, E.,

Salonen, J., Santos, H.A., 2017. Development and optimization of methotrexate-loaded lipid-polymer hybrid nanoparticles for controlled drug delivery applications. International Journal of Pharmaceutics. https://doi.org/10.1016/j.ijpharm.2017.09.061

Talegaonkar, S., Mittal, A., Parmar, S., Aqil, M., 2009. Aripiprazole loaded polymeric biodegradable microspheres: Formulation and in vitro characterization. Journal of Dispersion Science and Technology. https://doi.org/10.1080/01932690802701788

Tello, P., Santos, J., Calero, N., Trujillo-Cayado, L.A., 2024. Formulation and Characterization of Sustainable Algal-Derived Nanoemulgels: A Green Approach to Minimize the Dependency on Synthetic Surfactants. Polymers. https://doi.org/10.3390/polym16020194

Vandana, K., Kumar, V., Rathour, A., 2024. Advancements In Herbal-Nano Formulations : A Systematic Review 30, 11099–11109. https://doi.org/10.53555/kuey.v30i5.4901